

Room temperature synthesis of CdS nanoflakes for photocatalytic properties

A. N. Kadam · R. S. Dhabbe · M. R. Kokate ·
K. M. Garadkar

Received: 23 October 2013 / Accepted: 17 December 2013 / Published online: 27 February 2014
© Springer Science+Business Media New York 2014

Abstract Herein, we report, preparation of cadmium sulphide (CdS) nanoflakes at room temperature by simple arrested precipitation method. The synthesized CdS nanoflakes were characterized by various techniques such as X-ray diffraction, scanning electron microscopy, energy dispersive spectroscopy, Fourier transform-infrared spectroscopy, and UV–Visible spectrophotometer. Nanoflakes of CdS were found to be a mixed-phases composed of cubic and hexagonal with average crystallite size of 20 nm. Surface morphology of CdS seems to be nanoflakes. The absorption spectrum was slightly shifted to blue region as compared to the bulk, this indicates that synthesized material is smaller in size. The band gap energy was found to be 2.48 eV. The photocatalytic results reveals that CdS nanoflakes exhibits excellent photocatalytic performance for methyl orange (20 ppm) degradation, under sunlight and UV within 120 min (83 and 95 % respectively).

1 Introduction

The semiconductor nanoparticles has attracted much interest during the past decade, owing to their unique size dependent optoelectronic and catalytic properties [1]. Among II–VI, chalcogenides, cadmium sulphide (CdS) is an important semiconductor with direct band gap of 2.42 eV [2]. CdS is the best visible light active semiconductor photocatalyst [3], it is probably one of the most significant electronic and optoelectronic materials with

several prominent applications, such as, photocatalysis [4], solar cells [5], light emitting diodes [6], laser logic gates [7], transistors and photodetectors [8]. Among all these applications, photocatalysis is one of the key technologies to solve both energy as well as environmental problems. CdS is one of the most promising photocatalyst with better properties like band gap, fine optical transmittance, and appropriate band potentials under different thermodynamic conditions for photocatalytic redox reactions. The utilization of sunlight can be used as a light source for photocatalytic reactions, this make it an efficient photocatalyst [9, 10]. In the last few decades many studies have been reported for the synthesis of CdS, such as solid state method [11], chemical bath deposition [12], mechanical alloying process [13] and pyrolysis of single source precursor. Generally, these methods required high temperature (≈ 500 °C) with the use of toxic and highly sensitive compounds [14]. Therefore, it is of great significance to introduce effective synthesis pathways at low temperature, low cost, fast with well controlled size and shape for desired applications. Recently, many attempts have been made to develop material with various morphologies such as, cauliflower [15], leaf [16], nanobelt [17] etc. These shapes have special properties as compared normal shapes; although, the significant achievement in the fabrication of the desired nanoparticles is still great challenge to develop a facile strategy for the development of good photocatalyst. The different morphologies shows unique photocatalytic properties, which cannot be realized in spherical shape photocatalytic systems [18].

In the present investigation, it is demonstrated simple and inexpensive method for the synthesis of CdS nanoflakes, by simple arrested precipitation technique at room temperature. Moreover, to check the applicability of CdS nanoflakes the photocatalytic degradation of methyl orange

A. N. Kadam · R. S. Dhabbe · M. R. Kokate ·
K. M. Garadkar (✉)
Nanomaterials Research Laboratory, Department of Chemistry,
Shivaji University, Kolhapur 416004, India
e-mail: kmg_chem@unishivaji.ac.in

(MO) was studied. The effect of CdS loading on degradation of methyl orange under UV irradiation has been investigated to find out the optimum loading of catalyst. The kinetic studies of MO degradation were investigated under sunlight and UV light in the presence and absence of CdS nanoflakes.

2 Experimental

2.1 Materials

All the chemicals were used of analytical grade and used as it is without further purification. Cadmium acetate dehydrate (s d fine Chem Ltd. Mumbai, India), thiourea (Merck Pvt. Ltd., Mumbai, India), cetyl trimethyl ammonium bromide (CTAB, 99 %) (Spectrochem Pvt. Ltd., Mumbai, India), 25 % ammonia (Loba Chemie Pvt. Mumbai, India), and sodium dodecyl sulfate (SDS) (Thomas Baker Pvt. Ltd., Mumbai, India). All the solutions were prepared in millipore water obtained from millipore water system.

2.2 Preparation of CdS nanoflakes

For the preparation of CdS nanoflakes, 50 mL (0.1 M) cadmium acetate was taken in the 250 mL beaker, then the sufficient amount of mixed surfactant solution (CTAB + SDS 1 % each) was added with vigorous stirring at room temperature. In order to arrest the precipitation of CdS aqueous ammonia was used as the complexing agent. Furthermore dropwise controlled addition of 50 mL (0.1 M) thiourea was added as a sulphur source. Then obtained precipitate was washed several times with distilled water and ethanol to remove all the impurities. Finally, the material was dried at 60 °C for 2 h.

2.3 Characterization of the materials

The XRD of synthesized CdS was recorded on a Panalytical diffractometer with Cu K α radiation ($\lambda = 1.5406 \text{ \AA}$) as a X ray source, operated at 40 kV in the range of 2θ , 20°–80°. The average crystallite size of CdS was calculated by using Scherrer's formula. Fourier transform infrared spectrum (FT-IR) of CdS was recorded on spectrum-one (Perkin Elmer) in the range of 4,000–400 cm^{-1} using KBr pellet. The UV–Vis absorption spectrum of CdS was recorded with UV–Vis–NIR spectrophotometer (Shimadzu, Model UV-3600). The surface morphology of CdS nanoflakes was scanned by scanning electron microscope (SEM) (JEOL, JSM-6360) at various magnifications. To know the elemental composition of the CdS powder, the EDS was recorded by using SEM model JEOL 6360 connected with EDS.

2.4 Photocatalytic activity of CdS for methyl orange degradation

Photocatalytic performance of the synthesized CdS nanoflakes was tested for the degradation of methyl orange for both UV (A high-pressure Hg lamp 250 W) and natural sunlight. The series of experiments were performed by varying the catalyst amount from 0.25 to 1.5 g/dm^3 in 20 ppm MO solution. Prior to the irradiation, dye solution was stirred for 30 min in dark to ensure adsorption–desorption equilibrium between CdS and MO, then solution was exposed to light with constant stirring at room temperature. At particular time interval, a 3 mL of aliquot was collected and then centrifuged to separate photocatalyst. The clear solution was used to monitor the concentration of MO by recording the absorbance from 200 to 700 nm using UV–Vis–NIR spectrophotometer. To check the possibility of adsorption process, the photocatalytic activities of CdS nanoflakes without light were also performed.

3 Results and discussion

3.1 XRD pattern of CdS

The XRD pattern for CdS is shown in the Fig. 1. The pattern consist of twelve peaks within the region between 2θ , 20°–80°. The determined characteristics 2θ values and [hkl] planes are 25.29° [100], 26.54° [111], 29.01° [101], 31.46° [200], 37.57° [102], 44.3° [220], 51.63° [311], 53.78° [201], 54.86° [004], 61.31° [104], 65.90° [203], 70.76° [311], attributed to reflections of mixed phases of CdS (cubic and hexagonal) which is compared with JCPDS Card No. 10-454 and 01-077-2306 respectively. The comparison of X-ray diffraction (XRD) pattern of the CdS with JCPDS cards reveals the formation of mixed phases.

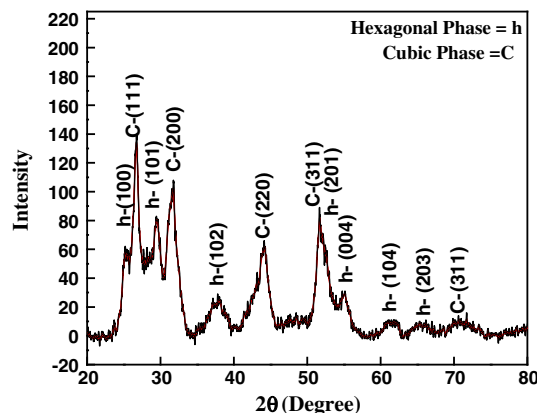


Fig. 1 The XRD pattern of CdS nanoflakes

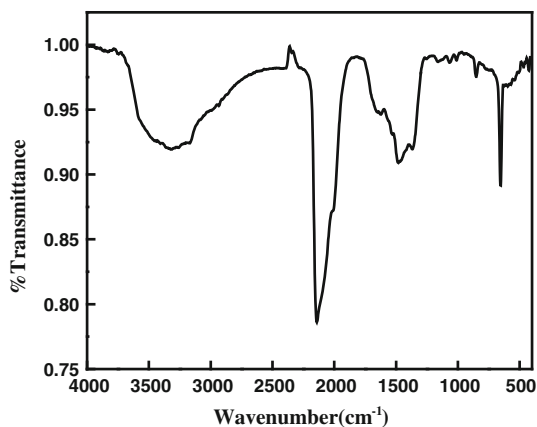


Fig. 2 FT-IR spectrum of CdS nanoflakes

The relatively broad peak width of the XRD pattern implies that the crystals are small in size [19]. The average crystallite size of CdS was calculated by using Scherrer's relation [20]

$$d = 0.9\lambda / \beta \cos \theta \tag{1}$$

where d is the average crystallite size, λ is wavelength of X-ray in Å, β is full width at half maximum [FWHM] in radian and θ is scattering angle in degree. The average crystallite size was found to be 20 nm.

3.2 FTIR spectrum of CdS

Figure 2 shows FT-IR spectrum of CdS, the band at $3,471\text{--}3,200\text{ cm}^{-1}$, which is attributed to OH stretching and band at $1,644\text{ cm}^{-1}$ is due to the OH bending mode of H_2O adsorbed on the surface of the CdS which may have crucial role in photocatalytic activity. The band at 643 cm^{-1} which is attributed to the Cd–S [21] stretching mode of vibrations, this confirmed the formation of CdS. The bands between $2,100$ and $2,200\text{ cm}^{-1}$ owing to the $\text{C}\equiv\text{N}$ stretching vibrations of thiocyanate is produced from the thiourea [22].

3.3 UV–Vis absorption spectrum of CdS

The UV–Vis absorption spectrum of CdS nanoflakes is shown in Fig. 3. According to the spectrum, the absorption edge is found to be in the visible region indicating the promising photocatalytic activity for both UV and sunlight. Moreover to know the material is either photocatalytic active in the UV or visible region, the band gap energy is important. The energy of light irradiation must be the greater than or equal to band gap energy of the semiconductor [23]. This criteria is useful for the formation of electron and hole pairs. The band gap is calculated by using the following relation:

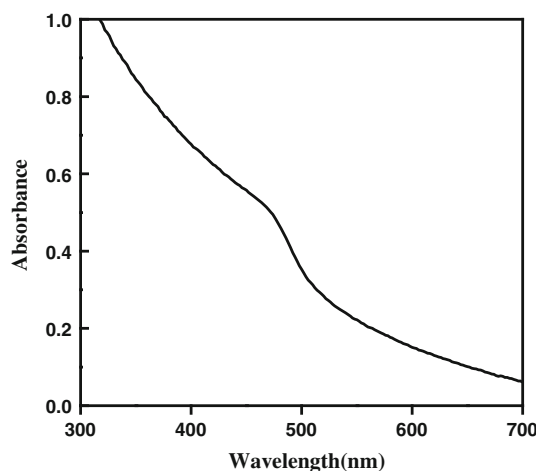


Fig. 3 Absorbance spectrum of CdS nanoflakes

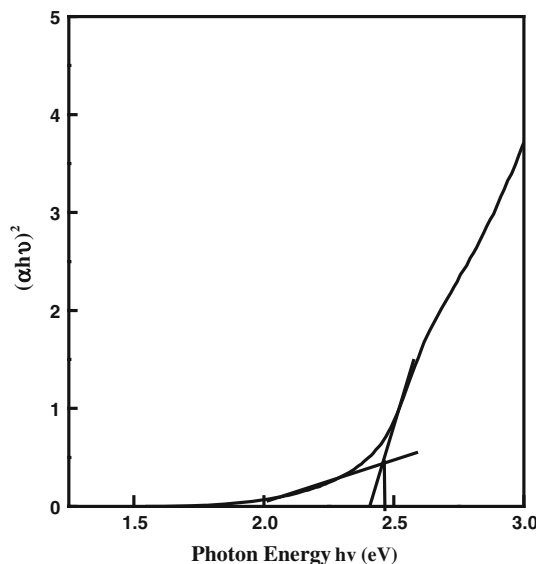


Fig. 4 A plot of $(\alpha hv)^2$ versus photon energy ($h\nu$)

$$\alpha hv = A(hv - E_g)^n \tag{2}$$

where $h\nu$ is the photon energy, α is the absorption coefficient, A is a constant for the material, and n is 0.5 for direct type of transition. The plot of $(\alpha hv)^2$ against the photon energy ($h\nu$) is shown in Fig. 4. The band gap was obtained by extrapolating the straight line to the $h\nu$ axis [24], which is found to be 2.48 eV.

3.4 SEM and compositional analysis

The surface morphology of the CdS was found to be CdS nanoflakes. The scanning electron microscopy images with different magnifications are shown in Fig. 5a, b. EDS was recorded in the binding energy region between 0 and

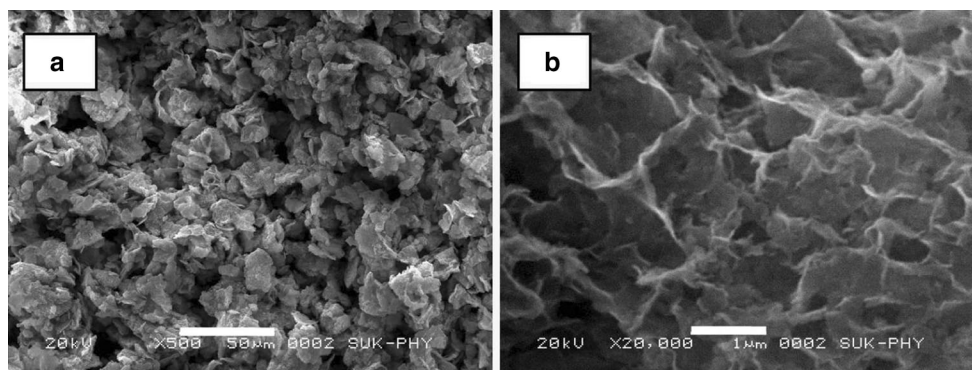


Fig. 5 SEM images of the CdS nano flakes at different magnifications **a** $\times 500$, **b** $\times 20,000$

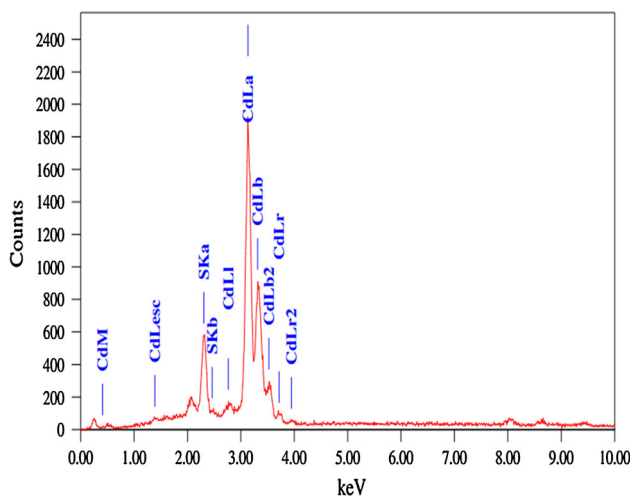


Fig. 6 EDS spectrum of CdS nanoflakes

10 keV which is shown in Fig. 6. The peaks of the spectrum reveals that presence of Cd and S at 3.13 and 2.30 keV respectively, which confirms the formation of CdS. The atomic % of cadmium and sulphur were found to be 60 and 40 % respectively, this indicated that synthesized CdS is cationic rich. The cationic rich CdS shows (n-type) very good photocatalytic performance in the form of heterojunction [25].

3.5 Factors affecting the photocatalytic degradation of methyl orange (MO)

The effects of natural sunlight and UV light (365 nm) on photocatalytic degradation of methyl orange are shown in Figs. 7 and 8 respectively. It is observed that there is no shift in the wavelength of MO during the course of photodegradation indicated that the photodegradation occurs without formation of toxic intermediate products i.e., mineralization of dye. For the sake of comparison, the photocatalytic activities of CdS nanoflakes were demonstrated under the following conditions. (1) Irradiation of the

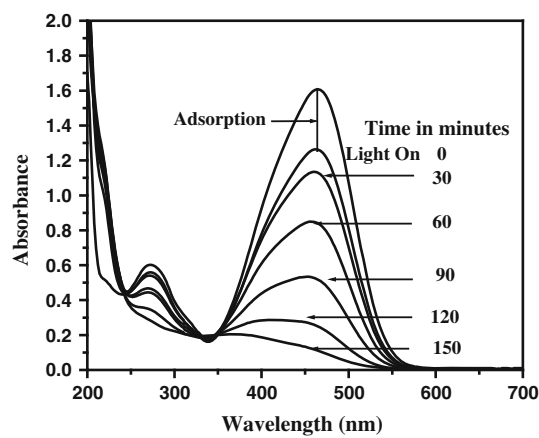


Fig. 7 Spectral changes of methyl orange over the CdS nanoflakes as a function of irradiation time under the sunlight

dye solution under sunlight and UV light in the absence of CdS, (2) the dye solution with CdS in dark and (3) irradiation of the MO solution under sunlight and UV light in the presence of CdS. The results of these studies are given in Fig. 9 which shows that direct photolysis did not cause any significant degradation for both under sunlight as well as UV irradiation. In the presence of CdS without irradiation, slight decrease in concentration of MO was observed this may be due to the adsorption of the dye on the surface of CdS. The irradiation under UV light in presence of catalyst caused 95 % degradation within 120 min where as 83 % was found under sunlight. This indicates that time required is more under the sunlight for degradation of MO. Wang et al. [26] reported on MO degradation at optimal conditions of 1.6 g/dm^3 catalyst, 10 ppm MO solution has obtained 83 % degradation efficiency under 300 W Xe-arc lamp within 80 min while in our case, 1.0 g/dm^3 catalyst even though double concentration of dye found to be more efficient (95 % within 120 min under UV light). While in case of natural sunlight a 83 % degradation efficiency was found within 120 min. This comparison shows that CdS nanoflakes synthesized at room temperature by arrested

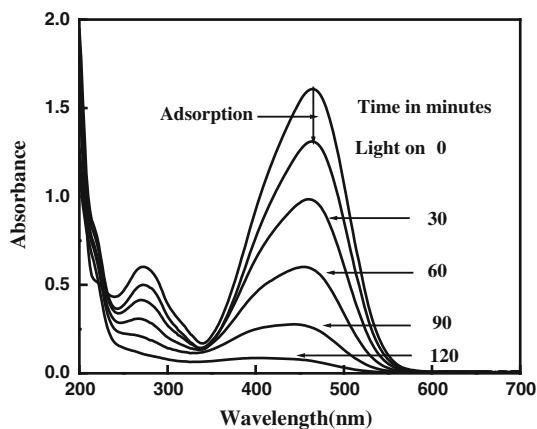


Fig. 8 Spectral changes of methyl orange over the CdS nanoflakes as a function of irradiation time under the UV light

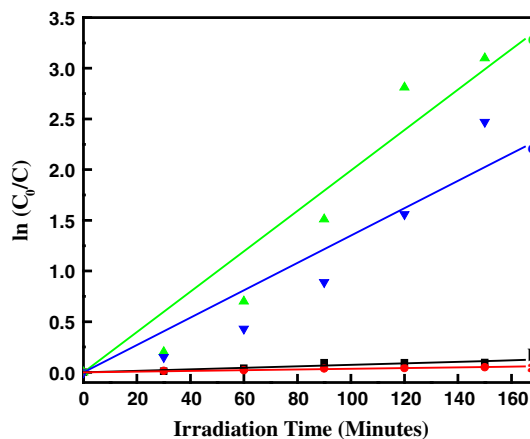


Fig. 10 The kinetic studies of MO degradation under, (a) sunlight, (b) UV light, (c) sunlight + CdS, (d) UV light + CdS

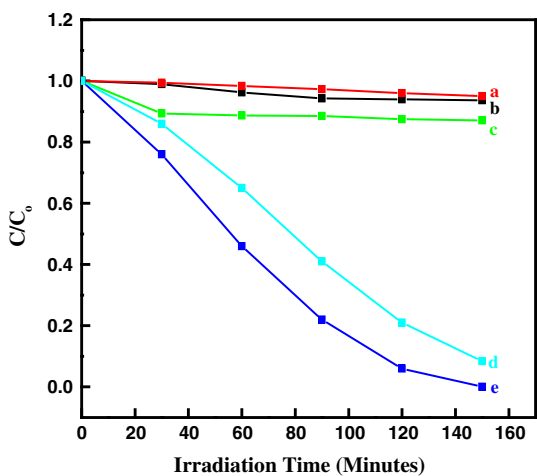


Fig. 9 The degradation efficiency of methyl orange under different conditions, (a) sunlight, (b) UV light, (c) adsorption in dark, (d) sunlight + CdS, (e) UV light + CdS

precipitation technique is seems to be more superior photocatalyst than the reported.

3.6 Kinetic studies

The kinetic studies of an aqueous MO dye degradation process plays an important role in assessing the efficiency and feasibility of treating dye from contaminated water. Therefore, the kinetic studies of MO degradation under sunlight and UV light has been discussed in the presence and absence of CdS. According to Langmuir–Hinshelwood (L–H) model [27], the rate expression at low initial concentration is given by

$$\ln(C_0/C_t) = kt \tag{3}$$

Table 1 Kinetic studies of degradation of methyl orange

Experimental conditions	Regression coefficient (R^2)	Rate constant (k) [min^{-1}]
UV light	0.9383	7.43×10^{-4}
Sunlight	0.990	3.55×10^{-5}
UV light + CdS nano-flakes	0.9719	1.984×10^{-2}
Sunlight + CdS nano-flakes	0.960	1.35×10^{-2}

where C_0 and C_t are the initial and concentration of the dye at time t respectively. The plot of $\ln C_0/C_t$ versus time for photodegradation is shown in Fig. 10. The linear fit between $\ln C_0/C_t$ and irradiation time supports the conclusion that the degradation follow first-order kinetics [28]. The values of regression coefficient (R^2) of the experimental runs were more than 0.93 indicating that the degradation of MO by the CdS satisfactorily followed an apparent-first-order kinetics [29]. The degradation efficiency of CdS in the presence of UV light was better than the sunlight. This may be due to the high energy of UV light in which rate of formation of electron hole pair is more. The values of rate constant and the regression coefficients are shown in the Table 1.

3.7 Effect of catalyst loading

The effect of CdS loading on the percentage degradation of the MO (20 ppm) dye under UV irradiation has been examined by varying the catalyst amount from 0.25 to 1.5 g/dm³ by keeping other parameters identical. The results shown in Fig. 11 indicate that the increase in catalyst loading from 0.25 to 1 g/dm³ increases the degradation efficiency from 35 to 95 % within 120 min. It can be seen that the degradation efficiency increases with the amount of catalyst

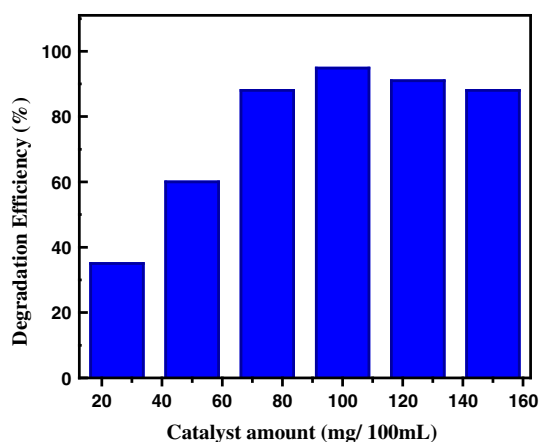


Fig. 11 Effect of catalyst loading on the degradation efficiency of methyl orange under UV irradiation within 120 min

loading, which is attributed to the increase in the number of active sites and more active sites will provide more chances to receive both light and guest molecules. Further increase in the catalyst loading does not affect the degradation efficiency significantly. This observation can be explained in terms of number of active sites available for photocatalytic reactions. It was found that large amount of catalyst may result in the agglomeration of catalyst, due to agglomeration active sites on the surface of catalyst becomes unavailable for photon absorption [30]. Another reason for the decreased degradation efficiency is turbidity of suspension which increases as the amount of photocatalyst increases this leads to decrease in penetration of UV light and hence activity of photocatalyst decreases [31, 32].

4 Conclusions

In the present investigation, CdS nanoflakes were successfully prepared at room temperature by arrested precipitation method. This method utilizes simple and inexpensive experimental set up. The mixed surfactants (CTAB + SDS 1 % each) were used as surface directing agent. The CdS was obtained in mixed phases containing cubic as well as hexagonal with average crystallite size of 20 nm. The EDS reveals that synthesized CdS is cationic rich which was resulted in improved photodegradation efficiency. The band gap is found to be 2.48 eV. The effect of photocatalyst loading, irradiation sources on the degradation of methyl orange was also examined. The photocatalytic results under UV and sunlight in the presence and absence of CdS showed the degradation of MO satisfactorily followed an apparent-first-order kinetics. The photocatalytic results reveals that CdS nanoflakes exhibits excellent photocatalytic performance for methyl orange (20 ppm), at 1 g/dm³. The degradation efficiency was

found to be 83 and 95 % within 120 min under sunlight and UV light respectively.

Acknowledgments One of the authors (A. N. K.) is thankful to DST-PURSE for providing fellowship and K. M. G. acknowledges to DST for providing Financial Assistance under the Major Research Project (SR/S1/PC/0041/2010).

References

1. B. Girginer, G. Galli, E. Chiellini, N. Bicak, *Int. J. Hydrogen Energy* **34**, 1176 (2009)
2. Y. Guo, J. Wang, Z. Tao, F. Dong, K. Wang, X. Ma, P. Yang, P. Hu, Y. Xu, L. Yang, *Cryst. Eng. Commun.* **14**, 1185 (2012)
3. D. Jing, L. Guo, *J. Phys. Chem. B* **110**, 11139 (2006)
4. W.M. Wu, G.D. Liu, Q.H. Xie, S.J. Liang, H.R. Zheng, R.S. Yuan, W.Y. Su, L. Wu, *Green Chem.* **14**, 1705 (2012)
5. P. Rodriguez, N.M. Aguirre, E.S.M. Martinez, G. Gonzalez, O. Zelaya, J. Mendoza, *Appl. Surf. Sci.* **255**, 740 (2008)
6. Z.L. Wang, *Mater. Sci. Eng.* **64**, 33 (2009)
7. P.C. Wu, Y. Ye, C. Liu, R.M. Ma, T. Sun, L. Dai, *J. Mater. Chem.* **19**, 7296 (2009)
8. J.S. Jie, W.J. Zhang, Y. Jiang, X.M. Meng, Y.Q. Li, S.T. Lee, *Nano. Lett.* **6**, 1887 (2006)
9. F. Chen, Y. Cao, D. Jia, X. Niu, *Ceram. Int.* **39**, 1511 (2013)
10. A.M. Abdulkarem, E.M. Elssfah, N.N. Yan, G. Demissie, Y. Yu, *J. Phys. Chem. Solids* **74**, 647 (2013)
11. S. Sohrabnezhad, A. Pourahmad, *J. Alloy. Compd.* **505**, 324 (2010)
12. J. Zhaeng, X.B. Song, M. Chen, X.G. Li, *Cryst. Growth Des.* **8**, 1760 (2008)
13. G.L. Tan, L. Zhang, X.F. Yu, *J. Phys. Chem.* **114**, 290 (2010)
14. Z.G. Li, J.H. Sui, X.L. Li, W. Cai, *Langmuir* **27**, 2258 (2011)
15. S. Rengaraj, S. Venkataraj, S.H. Jee, Y. Kim, C.W. Tai, E. Repo, A. Koistinen, A. Ferancova, M. Sillanpaa, *Langmuir* **27**, 352 (2011)
16. X. Fu, J. Liu, Y. Wan, X. Zhang, F. Meng, J. Liu, *J. Mater. Chem.* **22**, 1782 (2012)
17. S. Xiong, X. Zhang, Y. Qian, *Cryst. Growth Des.* **9**, 5259 (2009)
18. S. Xiong, B. Xi, Y. Qian, *J. Phys. Chem. C* **114**, 14029 (2010)
19. R. Seoudi, A.A. Shabaka, M. Kamal, E.M. Abdelrazek, W. Eisa, *Phys. E* **45**, 47 (2012)
20. G. Li, D. Zhang, J.C. Yu, *Environ. Sci. Technol.* **43**, 7079 (2009)
21. Z.R. Khan, M. Zulfeqar, M.S. Khan, *J. Mater. Sci.* **46**, 5412 (2011)
22. Y. Yu, Y. Ding, S. Zuo, J. Liu, *Int. J. Photoenergy* (2011). doi:10.1155/2011/762929
23. X. Chen, S.S. Mao, *Chem. Rev.* **107**, 2891 (2007)
24. K.M. Garadkar, A.A. Patil, P.P. Hankare, P.A. Chate, D.J. Sathe, S.D. Delekar, *J. Alloy. Compd.* **487**, 786 (2009)
25. Y. Bessekhouad, D. Robert, J.V. Weber, *Photochem. Photobiol. A: Chem.* **163**, 569 (2004)
26. D. Wang, D. Li, L. Guo, F. Fu, Z. Zhang, Q. Wei, *J. Phys. Chem. C* **113**, 5984 (2009)
27. I.K. Konstantinou, T.A. Albanis, A review. *Appl. Catal. B: Environ.* **49**, 1 (2004)
28. S.K. Mohapatra, N. Kondamudi, S. Banerjee, M. Misra, *Langmuir* **24**, 11276 (2008)
29. H. Li, G. Wang, F. Zhang, Y. Cai, Y. Wang, I. Deerdj, *RSC Adv.* **2**, 12413 (2012)
30. O.K. Mahadwad, P.A. Parikh, R.V. Jasra, C. Patil, *Bull. Mater. Sci.* **34**, 551 (2011)
31. N. Guetta, H.A. Amar, *Desalination* **185**, 427 (2005)
32. P.V. Korake, R.S. Dhabbe, A.N. Kadam, Y.A. Gaikwad, K.M. Garadkar, *J. Photochem. Photobiol. B* **130**, 11 (2014)